Vapor pressure measurements over supercooled water in the temperature range from 10 1 °C to +10 2 °C

VAPOR PRESSURE MEASUREMENTS OVER SUPERCOOLED WATER IN THE TEMPERATURE RANGE FROM -10^{1} °C TO $+10^{-2}$ °C

Authors: G. Beltramino, L. Rosso, D. Smorgon, V. Fernicola

Affiliation: INRIM - Istituto Nazionale di Ricerca Metrologica, Torino, Italy

Corresponding author: G. Beltramino (g.beltramino@inrim.it)

Abstract

An accurate measurement of saturation vapor pressure of supercooled water is a strong challenge in metrology, mainly due to difficulties concerning keeping water at a liquid state at temperatures well below the melting point; thus few experimental data covering limited temperature ranges (down to about 253 K) are reported in literature. For this reason , an investigation of the water vapor – supercooled water equilibrium along the saturation line is carried out at Istituto Nazionale di Ricerca Metrologica (INRIM).

Measurements cover the temperature range from 261.26 K to 273.25 K, corresponding to a saturation vapor pressure from about 244 Pa to 611 Pa. The experimental apparatus includes a pyrex sample cell, kept in a liquid bath at a constant temperature with a millikelvin stability and connected to a manifold where the pressure is measured using one capacitive diaphragm pressure gauge.

In this work, the water sample preparation, the measuring method and measurement corrections are reported; moreover, a comparison between experimental and literature data is conducted along with the most used vapor pressure formulations. Measurement results are discussed and uncertainty sources estimated. The resulting expanded relative uncertainty (k = 2) varies from 0.058 % at 273.25 K to 0.160 % at 255.26 K.

Keywords *Supercooled water–water vapor equilibrium ; Clapeyron equation ; Saturation vapor pressure ; Static measurements method ; Water properties*

1. Introduction

Determination of saturation vapor pressure over supercooled water plays an important role in atmospheric processes, because high altitude clouds (like cirrus and polar stratospheric clouds) can contain not only ice particles but also water droplets at temperature down to about 230 K.
The vapor pressure of supercooled water is necessary for calculations of the nucleation and growth of water and ice droplets in the atmosphere; furthermore it can be used to calculate the latent heat, which is valuable in modeling weather formations.
The supercooling of aqueous salt solutions is important because there are claims that supercooling occurs in ocean waters [1].
In literature many vapor pressure equations over liquid water are present, although they are valid only for temperatures above 273.15 K; under the melting point, in which liquid water is present in a supercooled state, the equations differ significantly.
This high uncertainty about the estimation of vapor pressure of supercooled water is due to a lack of experimental data, which have a limited covering temperature range (down to about 235 K, which is the limit of homogenous nucleation), because of difficulties inherent in measuring properties of metastable states.
On the other hand, the measurements of the vapor pressure of ice reach now a high level of accuracy, with relative standard uncertainty between 0.4 % and 0.7 % over the temperature range 175 K to 253.4 K [2].

Murphy and Koop [3] developed an equation of the vapor pressure for supercooled liquid water, using the knowledge of the specific heat at constant pressure c_p above 233 K and its asymptotic trend at the temperature limit of amorphous ice (130 K – 150 K). This equation was compared with other ones [9-16] and with existing experimental data [4-6,8], except for the range of temperatures between 150 K and 232 K (called the "no-man's land") in which experimental data are missing.
In the twentieth century, the first available vapor pressure data of supercooled water were provided by Scheel and Heuse (1909) [4], who were able to maintain a supercooled state at temperatures below the melting point down to about 258 K.
Much more accurate measurements were conducted by Bottomley [5] in 1978, covering about the same temperature range as Scheel and Heuse. At a constant temperature, he measured the difference in vapor pressure between supercooled liquid and stable ice, connecting the two samples of water (at liquid and solid phase) to each side of a differential pressure transducer.
Kraus and Greer (1984) [6] were able to make measurements at temperatures down to 251 K by means of vapor condensation into a cold cell so as to form many droplets on the cell surfaces. But the resulted anomalously low vapor pressures below 254 K suggested the partial freezing of the droplets in this temperature range, making the measurements unreliable.
Fukuta and Gramada (2003) [7] carried out vapor pressure measurements over a larger temperature range, down to 243 K, measuring the temperature difference necessary to equalize the vapor pressure of a small supercooled droplet of water at one temperature and ice at another higher value. They monitored the equilibrium between the droplet and the ice reservoir observing the size of the droplet by means of an optical microscope.

Cantrell et al. (2007) [8], similarly to Fukuta and Gramada, monitored a thin film of water in equilibrium with an ice reservoir using attenuated total reflection infrared spectroscopy. This technique enabled them to detect submonolayer changes in film thickness and ensured to measure the vapor pressure of water, not a mixture of water and ice. They were able to carry out vapor pressure measurements of supercooled water from the melting point to 260.15 K.

The empirical equations that put in a direct relationship saturated vapor pressure and temperature, allowing also the calculation of other humidity quantities such as relative humidity and water vapor mole fraction, are based on the Clapeyron equation:

$$\mathrm{d}p/\mathrm{d}T = \Delta s/\Delta v\,, \tag{1}$$

where Δs is the difference in the molar entropies between vapor and liquid state of water and Δv is the difference in the molar volumes.
The reversibility of the phase transition supercooled liquid-vapor implies that the difference in the molar entropies can be associated with a definite amount of heat, $\Delta s = L_{\mathrm{liq}}/T$, where L_{liq} is the latent heat of vaporization at temperature T.
If the gas is ideal (water vapor can be considerate, with excellent approximation, as ideal-gas in the atmospheric temperature/pressure range) and the molar volume of the vapor is much greater than of the liquid, the Clapeyron equation can be manipulated into the so called Clausius-Clapeyron equation:

$$\mathrm{d}p/\mathrm{d}T = L_{\mathrm{liq}}p/RT^2, \tag{2}$$

where R is the molar gas constant.
The integration of this equation can start at the triple-point of water (pressure p_{t} = (611.657 ± 0.01) Pa and temperature T_{t} = 273.16 K).
Calculation of L_{liq} can be done from the knowledge of this quantity at temperature T_{t}, then using the difference in the molar heat capacities of the supercooled liquid $c_{p,\mathrm{liquid}}$ and vapor $c_{p,\mathrm{vapor}}$, in order to obtain the other values through Kirchhoff's relation:

$$\mathrm{d}L_{liq}/\mathrm{d}T \approx \Delta c_p(T), \tag{3}$$

where $\Delta c_p = c_{p,\mathrm{liquid}} - c_{p,\mathrm{vapor}}$.

The relationship temperature – saturated vapor pressure (in equilibrium with respect to both ice and supercooled water) can be obtained also starting from the development of a Gibbs energy function $g(T,p)$ of temperature and pressure, from which many others thermodynamic equilibrium properties can be derived by means of partial derivatives.
Feistel and Wagner [17] developed an equation of state for hexagonal ice valid over a wide range of pressures and temperatures; the equation is based on an extension of previously developed Gibbs functions, covering the entire existence region of ice Ih in the T-p diagram.

A similar Gibbs energy function that allows to derive the saturated vapor pressure dependence on temperature, in equilibrium with respect to supercooled water, was provided by Holten et al. [18], using the phase-equilibrium condition:

$$g(T, p_\sigma) = g_{\mathrm{vap}}(T, p_\sigma), \tag{4}$$

where g_{vap} is the specific Gibbs energy of water vapor, which was calculated from the IAPWS-95 formulation.

At INRIM, an investigation of the vapor-supercooled liquid equilibrium along the condensation line is carried out. Measurements cover the temperature range from 261.15 K to 273.15 K, which is similar to those ones explored in the previous studies, because of difficulties inherent in maintaining water at a supercooled state with temperatures lower than 258.15 K, for a period long enough in order to have reliable saturated vapor pressure values. The aim is to provide more accurate saturated vapor pressure measurements, lowering the high uncertainty that still affects them.

In this paper the experimental apparatus is described and a comparison between experimental data and results from previous studies [4-6,8] and calculated values by known formulations [9-16,18] is provided. Error correction terms and measurement uncertainty sources, including thermal transpiration and hydrostatic pressure head, are discussed and evaluated.

2. Measurement method and experimental apparatus

In this work, the experimental determination of saturated vapor pressure is based on a static method of pressure measurement inside a cell partially filled with water, kept at a supercooled state over the whole temperature range of study. After being sure that no volatile components are present inside the system between the pressure gauge and the measurement cell, except for water vapor, the total pressure reaches a value equal to the saturated vapor pressure in equilibrium with liquid water, at a fixed cell temperature. At this condition, just above the air-liquid interface, the evaporation rate of liquid water is perfectly balanced by the condensation rate of water vapor, so that the total amount of water molecules at gaseous state remains constant.
The experimental apparatus, shown in Fig. 1, consists of:

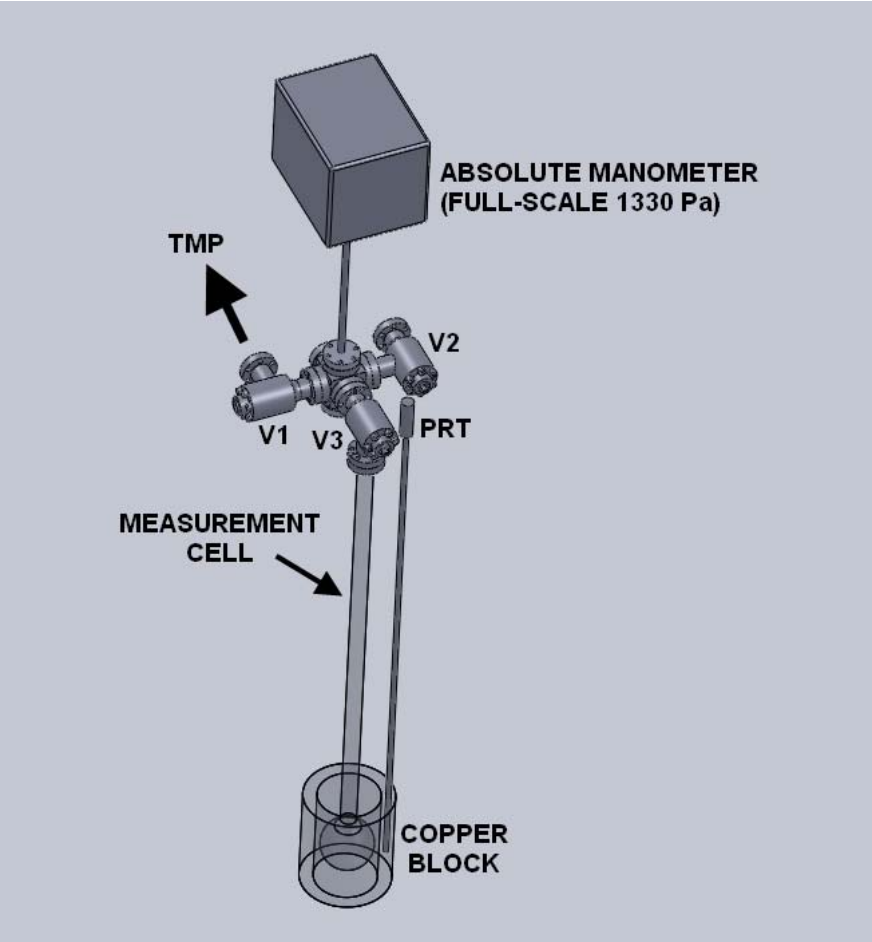

Fig. 1 . *Experimental apparatus for the measurement of water vapor pressure over supercooled water.*

- A borosilicate glass sample cell, 500 mm long with external diameter of 15 mm and wall thickness of 1 mm. The cell is immersed in a calibration bath filled with alcohol. The temperature of the cell is measured by means of a platinum resistance thermometer (PRT) placed inside a copper block that wrap the bulb, to a depth such that the sensible element is situated at the same level of the water-air interface inside the cell.

- One capacitive diaphragm pressure gauge to measure the vapor pressure.

- A turbomolecular pump (TMP) to maintain a high level of vacuum inside the system.

The capacitance manometer is connected to the same inlet of a six-port manifold at the top of the sample cell, which is immersed in a calibration bath. A turbo-molecular pump (TMP) is also connected to one inlet of the manifold. Three bakeable UHV valves isolate each part of the system (V2 is the access port for further instrumentation, e.g. MS-RGA).

The pressure gauge is a precision absolute capacitance manometer with full scale pressure range of 1330 Pa. It's equipped with heating base, in order to keep the sensor at a constant temperature of about 45 °C, and is connected to the measurement cell through a six-port manifold, also heated at the same temperature of the manometer in order to minimize the thermal transpiration effect. The gauge is mechanically decoupled by anti-vibration pads.
The sample cell has a cylindrical shape with a terminating 60 mm – diameter bulb, filled with about 1 ml of distilled water, taken from a commercial ultra-pure water source which ensures an electrical conductance of the water of not more than 0.7 $\mu S\ cm^{-1}$. This very little amount of water can increase the probability to keep it at a supercooled state at temperatures well below 273.15 K.
In order to remove dissolved impurities from the sample, which can promote earlier water freezing and compromise the measurement accuracy, several cycles of water freezing, followed by pumping by means of the turbo-molecular pump (TMP), and then thawing again under low pressure are performed. The cycles (4-to-6) are repeated until the residual pressure in the cell below 5×10^{-6} Pa is measured.
The sample cell is placed, together with the cylindrical copper block, in a commercial calibration bath with an operating temperature range from 193.15 K to 383.15 K. The bath tank is 400 mm deep with a 18 l capacity; its temperature stability declared by the constructor is ±6 mK at 193.15 K when ethanol is used as the working fluid. The copper block improves the temperature stability and uniformity around the bulb, measured by means of the calibrated platinum resistance thermometer (PRT) inserted into the thermowell in the copper block.

Two saturation vapor pressure measurements cycles in equilibrium with supercooled water are carried out, starting from a bath temperature of 261.15 K, the lowest temperature achievable with water sample kept at a supercooled state, and increasing bath temperature in steps of 1 K up to 273.15 K. Between the cycles, in order to reduce zero drift of the manometer, the residual gas into the system (except the sample cell) is pumped out until reaching the maximum vacuum degree allowable using the TMP.
At the end of the two measurements cycles, a triple point of water (TPW) is realized in the sample cell, obtaining a saturation vapor pressure, measured by the manometer, of (614.155 ± 0.02) Pa; correcting the raw pressure reading taking account for manometer calibration, thermal transpiration and hydrostatic pressure head, the value is 611.654 Pa, which is very close to the widely-accepted best estimate value (611.657 Pa) from [19].
It is observed that the pressure value remains constant during a stable interval time of bath temperature, without any positive trend due to an external leakage of the system (ambient air that enters somewhere between the cell and the pressure gauge). So the leakage is negligible and it's not necessary to bring about any corrections to compensate for it.

As done with the triple-point of water, all the raw pressure readings of the manometer are corrected for gauge calibration, thermal transpiration effect and hydrostatic pressure head, adding also the correction for the TPW measured.

Table 1 shows the percent relative corrections applied on pressure measured values. to obtain the corrected values of vapor pressure over supercooled water.. The corrections applied are the manometer's calibration, the hydrostatic head, the thermal transpiration effect and the adjustment to the TPW pressure measured during the experimental measurements.

	Percent pressure corrections (10^2 $\Delta p/p$) / Pa			
***T* / K**	**Hydrostatic head**	**Pressure gauge calibration**	**Thermal transpiration**	**Adjustment to TPW**
261.255	0.006	-0.456	-0.001	0.001
262.254	0.006	-0.451	-0.001	0.001
263.251	0.006	-0.447	0.000	0.001
264.246	0.006	-0.443	0.000	0.001
265.250	0.006	-0.439	0.000	0.001
266.248	0.006	-0.435	0.000	0.001
267.240	0.006	-0.431	0.000	0.001
268.242	0.006	-0.428	0.000	0.001
269.242	0.006	-0.425	0.000	0.001
270.250	0.006	-0.422	0.000	0.001
271.248	0.006	-0.419	0.000	0.001
272.248	0.006	-0.416	0.000	0.001
273.251	0.006	-0.413	0.000	0.001

Table 1 *Percent corrections applied to the pressure gauge raw readings taking account of calibration, hydrostatic head, thermal transpiration and adjustment of the triple point of water.*

The hydrostatic head correction corresponds to the gas column (total height of (870 mm ± 10 mm) between the liquid-vapor interface and the pressure gauge. The column is divided into two parts (410 mm and 460 mm) whose temperatures are respectively 45 °C and the sample temperature, supposing that a step-profile temperature is present (instead of a more real fast but non sudden temperature change). The hydrostatic head is calculated using the hypsometric equation:

$$p_1 \,/\, \mathrm{Pa} = p_0 \,/\, \mathrm{Pa} \times \left(e^{\frac{g}{R_v} \times \left(\frac{\Delta z_2}{T_{sample} \,/\, K} + \frac{\Delta z_1}{T_{man}} \right)} - 1 \right). \quad (5)$$

In this equation:

p_1 is the pressure at the interface liquid-vapor;
p_0 is the pressure measured by the manometer;
g is the local gravity (9.810874 m s^{-2});
R_v is the specific gas constant for water vapor (461 J kg^{-1} K^{-1});
T_{man} is the pressure transducer temperature (318.15 K);
T_{sample} is the sample temperature;
Δz_2 is the length of the gas column at temperature $T = T_{sample}$ and Δz_1 is the length of the gas column at $T = T_{man}$. The quantities Δz_1 and Δz_2 are a length of 460 mm and 410 mm respectively.

The hydrostatic head contribution to the whole applied correction on pressure values can be considered negligible over the whole measurement range, adding only 20-30 mPa to the raw pressure gauge readings.

The thermal transpiration effect creates a pressure difference between the capacitance manometer and the sample when the pressure transducer is heated at a temperature above the ambient one and the pressure in the system is at a pressures lower than 100 Pa. For free molecular flow, that means when the mean free path among molecules is large compared with the connecting tube diameter, kinetic theory predicts that the temperature difference between the sample (T_s) and the pressure transducer (T_g) causes a gauge pressure (p_g) that is higher than the sample pressure (p_s), with a ratio that can be expressed as $p_g/p_s = (T_g/T_s)^{1/2}$. For pressures between the molecular-flow regime limit and the high-pressure regime, where $p_g = p_s$, empirical equations are used to calculate the correction due to the thermal transpiration effect. In this work, the thermal transpiration effect is calculated by means of the Takaishi-Sensui [20] equation and Yasumoto [21] coefficients. However, the amount of this effect is negligible in the temperature range explored, because it starts to become relevant at pressures lower than 100 Pa, that corresponds at saturation vapor pressures relative to temperatures below 250 K.

3. Experimental results

Table 2 lists the measured vapor pressures over supercooled water at the corresponding temperatures, including the estimated expanded (k = 2) uncertainties. Only data regarding the second measurement cycle are present, but it can be indifferent to choose the first one or to take mean values between the two cycles, because at each temperature the difference between them is always within its uncertainty, making a cycle indistinguishable from the other one.
Figure 2 compares present and past experimental results taken from the literature, showing in the y-axis the vapor pressure relative to that one calculated in equilibrium with ice, at the same temperature, by means of the IAPWS 2011 formulation [22].

Figure 3 compares the present experimental results with the calculated vapor pressures over supercooled water as obtained from several empirical formulations [9-16]; Murphy & Koop's formulation is used as the reference.
Most of these formulations, including the IAPWS one published in 2002, are valid only above the triple point, so results below this temperature represent an extrapolation outside the range of validity of the formulations.

T / K	U(*T*) / K	*p* / Pa	U(*p*) / mPa	U(*p*)/*p* / %
261.255	0.002	246.2	210	0.085
262.254	0.002	266.7	212	0.079
263.251	0.002	288.6	214	0.074
264.246	0.002	312.2	216	0.069
265,250	0.002	337.6	218	0.065
266.248	0.002	364.7	220	0.061
267.240	0.002	393.7	223	0.057
268.242	0.002	424.7	227	0.053
269.242	0.002	458.0	231	0.050
270.250	0.002	493.9	235	0.048
271.248	0.002	531.8	238	0.045
272.248	0.002	572.4	239	0.042
273.251	0.002	615.8	239	0.039

Table 2 *Experimental measurements and associated expanded uncertainty (k=2) of the saturation vapor pressure over super-cooled water in the temperature range from 261.26 K to 273.25 K.*

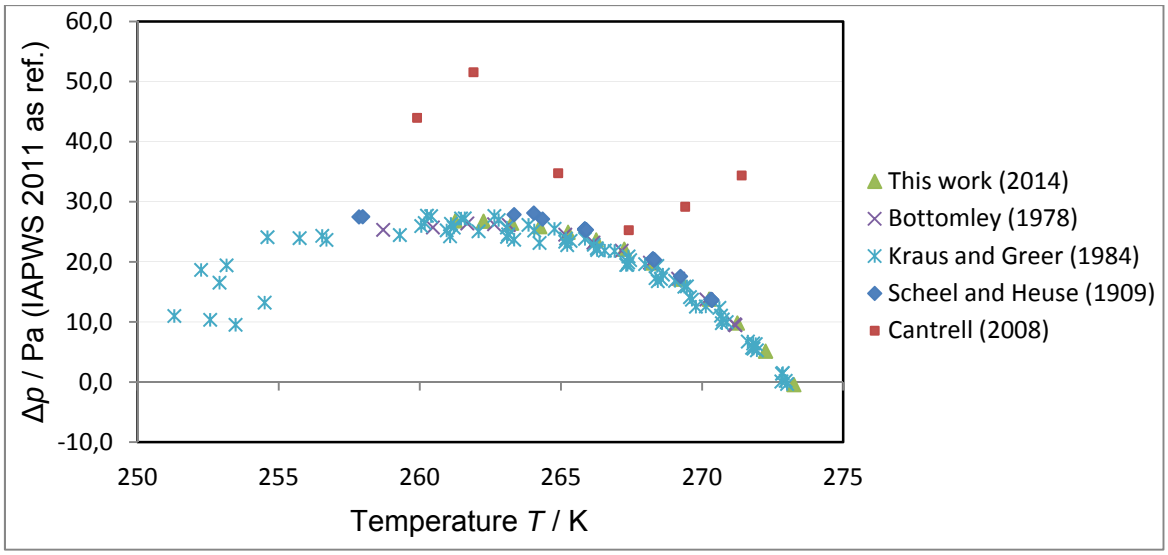

Figure 2 *Comparison of the experimental measurements reported in this work with those previously published. To obtain homogeneity between them, all data are referred to the saturation vapor pressure over ice as calculated using IAPWS 2011 formulation.*

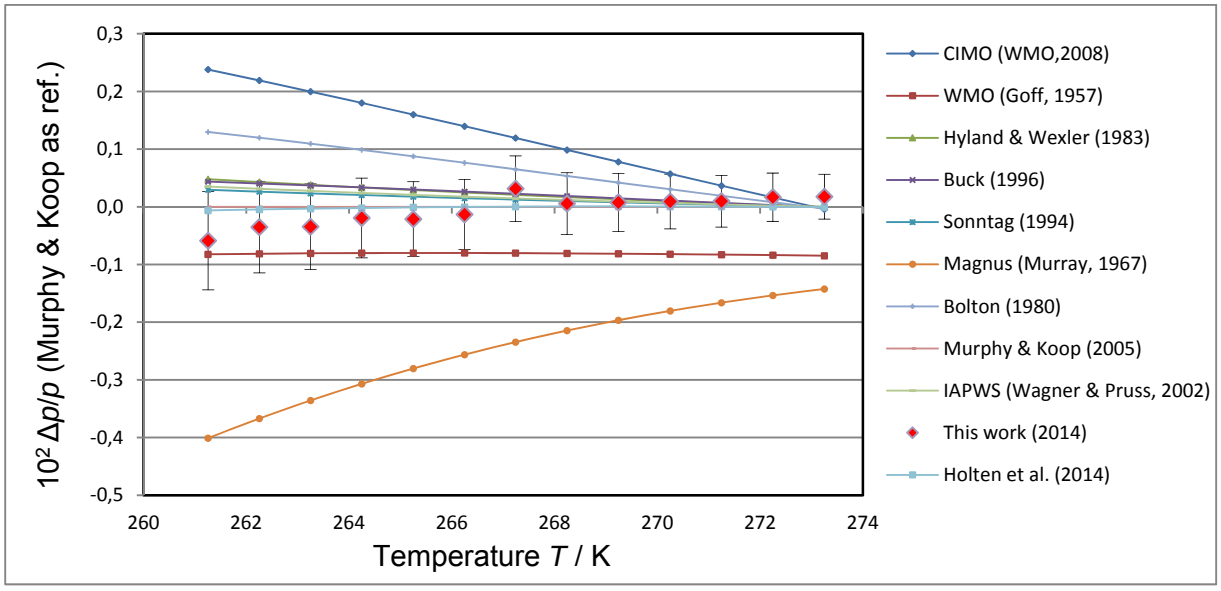

Figure 3 *Comparison between several formulations for saturation vapor pressure over supercooled water, including experimental data of this work with respective uncertainty bars (k=2). Murphy & Koop's formulation is used as a reference. The deviations of the values calculated using Goff, 1957 and Murray, 1967 near the melting point, with respect to the other formulations and the experimental data, are due to the old value of the vapor pressure at the triple point of water that was slightly lower than the recent one.*

Table 3 reports the estimate of the most significant contributions to the total temperature uncertainty budget, at the temperature of 263 K (corresponding to a vapor pressure of about 288 Pa).

The first two uncertainty components (thermometer calibration and resistance bridge linearity) are constant over the whole range, depending on the overall instrument behavior over its working range, while the last two, regarding bath temperature stability and uniformity, are calculated from experimental data made at the specific temperature. The largest contributions come from bath stability and uniformity. The overall measurements standard uncertainty is not higher than 1 mK over the whole range of study, because the uncertainty related to the bath decreases with increasing temperature from 263 K to 273.16 K.

Uncertainty source	***Temperature measurement uncertainty*** **u(*T*) / mK**
SPRT calibration	0.20
Resistance bridge linearity	0.58
Bath temperature stability	0.79
Bath temperature uniformity	0.81
Combined standard uncertainty	1.06

Table 3 *Standard uncertainty components (k=1) of temperature measurements at 263 K, corresponding to a water vapor pressure of ~288 Pa.*

Table 4 lists the uncertainty sources regarding pressure measurements uncertainty. The largest of them is due to the manometer calibration, followed by the realization of the triple point of water in the sample cell. The gauge zero, together with the span drift and linearity, has also a non-negligible contribution to the uncertainty budget, while the contributions given by hydrostatic head and thermomolecular effect corrections are of minor importance. The value of the residual gas effect is taken from [23], because it has been previously measured accurately by means of a mass-spectroscopy residual gas analyzer (MS RGA), mounted on-line in an experimental apparatus very similar to this one.

Uncertainty source	***Pressure measurement uncertainty*** **u(*p*) / mPa**
TPW realization	26.51
Calibration	102.02
Zero and span drift (2 ppm F.S./day)	3.10
Hydrostatic head correction	0.19
Thermomolecular effect correction	0.60
Residual gas effect	0.32
Combined standard uncertainty	107.02

Table 4 *Measurement uncertainty components and combined standard uncertainty (k=1) of pressure measurements at ~288 Pa.*

4. Conclusions

An investigation of the liquid-vapor equilibrium along the condensation line at negative temperatures is carried out at INRIM. A static vapor pressure measurement method using a diaphragm pressure gauge is used to explore a temperature range in which liquid water can remain at a supercooled state (from the melting point of water down to 261.26 K).
The experimental apparatus consists of a calibration bath, in order to control the temperature of the sample cell, an absolute capacitive pressure gauge (F.S. 1330 Pa) for vapor pressure measurements and a capsule PRT-type for sample temperature measurements.
Potential sources of uncertainty, (thermal transpiration, hydrostatic head, manometer calibration, TPW realization, gauge zero and span drift and residual gas effect) are considered.
Over all the temperature range explored in this work, the sum of the uncertainty contributions from manometer calibration and TPW realization covers more than 95 % of the overall pressure measurement uncertainty, while the others sources of uncertainty are negligible. No leakage effect is observed during the experimental test, letting pressure measurement be stable with a stable bath temperature, without any positive trend due to infiltration of ambient air inside the system.
The experimental results compare favorably with past measurements and most of the recent vapor pressure formulations over supercooled water, over the temperature range explored. A relative expanded uncertainty (k=2) from 0.039 % to 0.085 % is obtained over the experimental range, which is lower than those ones resulted from previous experimental works. As an example, regarding vapor pressure data from Kraus and Greer [6], the accuracy of the manometer (about 3 Pa) is already higher than the overall uncertainty of the experimental apparatus used in this work.
A slightly different experimental apparatus, using a capillary tube as sample cell, can allow to maintain water at liquid state at temperatures lower than 261.15 K, so that it can be possible to make vapor pressure measurements of supercooled water over a wider temperature range.

Acknowledgments We gratefully acknowledge M. Banfo for its assistance in assembling the measurement setup.

5. References

[1] S.C. Greer, *Investigation of the Thermodynamics of Supercooled Water and Supercooled Saline Water*, National Bureau of Standards Washington D.C. (1979).

[2] K. Bielska, D. K. Havey, G. E. Scace, D. Lisak, A. H. Harvey, J. T. Hodges, *High-accuracy measurements of the vapor pressure of ice referenced to the triple point*, Geophysical Research Letters **40**, 6303 (2013), doi:10.1002/2013GL058474.

[3] D.M. Murphy, T. Koop, Q. J. Meteorol. Soc. **131**, 1539 (2005), doi:10.1256/qj.04.94.

[4] K. Scheel, W. Heuse, W. Ann. Phys. **29**, 723 (1909).

[5] G. Bottomley, Austr. J. Phys. **31**, 1177 (1978).

[6] G. Kraus, S. Greer, J. Phys. Chem. **88**, 4781 (1984).

[7] N. Fukuta, C. Gramada, J. Atmos. Sci. **60**, 1871 (2003),doi:10.1175/1520-0469(2003)060<1871:VPMOSW>2.0.CO;2.

[8] W. Cantrell, E. Ochshorn, A. Kostinski, K. Bozin, *Measurements of the vapor pressure of supercooled water using infrared spectroscopy*, J. Atmos. Oceanic Technol. **25**, 1724 (2008); **26**, 853 (2009), doi:10.1175/2008/JTECHA1028.1.

[9] R.W. Hyland, A. Wexler, Trans. Am. Soc. Heat. Refrig. Air Cond. Eng. **89**, 500 (1983).

[10] *Buck Research Manual* (1996).

[11] F.W. Murray, J. Appl. Meteorol. **6**, 203 (1967).

[12] D. Bolton, Monthly Weather Review **108**, 1046 (1980).

[13] J. A. Goff, *Transactions of the American Society of Heating and Ventilating Engineers*, 347–354 (1957).

[14] D. Sonntag, Z. Meteorol. **3**, 51 (1994).

[15] W. Wagner, A. Pruß, J. Phys. Chem. Ref. **31**, 387 (2002), doi:10.1063/1.1461829.

[16] *CIMO Guide*, WMO-No. 8 (2008).

[17] Feistel R. and W. Wagner, *A new equation of state for H2O ice Ih*, J. phys. chem. ref. data **35**:
1021-1047 (2006), doi:10.1063/1.2183324.

[18] V. Holten, J. V. Sengers, M. A. Anisimov, *Equation of state for supercooled water at pressure up to 400 MPa*, J. phys. chem. ref. data **43**, 043101 (2014), doi:10.1063/1.4895593.

[19] L.A. Guildner, D.P. Johnson, F.E. Jones, J. Res, Natl. Bur. Stand. **80**, 505 (1976), doi:10.6028/jres.080A.054.

[20] T. Takaishi, Y. Sensui, Trans. Faraday Soc. **59**, 2503 (1963).

[21] I. Yasumoto, J. Phys. Chem. **84**, 589 (1980).

[22] IAPWS, *Revised Release on the Pressure along the Melting and Sublimation Curves of Ordinary Water Substance* (2011), http://www.iapws.org.

[23] V. Fernicola, L. Rosso, M. Giovannini, Int J Thermophysics **33**, 1363 (2012), doi:10.1007/s10765-011-1128-2.